

# Digital Image-Based Colorimetry Utilizing Gold Nanoparticles (AuNPs): Portable Quantitative Detection of Cd<sup>2+</sup>

Eduwin Saputra and Sri J. Santosa\*

Departement of Chemistry, Faculty of Mathematics and Natural Sciences, Universitas Gadjah Mada, Yogyakarta, Indonesia  
Email: eduwinsaputra@mail.ugm.ac.id (E.S.); sjuari@ugm.ac.id (S.J.S.)

\*Corresponding author

Manuscript received April 22, 2024; revised May 21, 2024; accepted July 11, 2024; published August 13, 2024

**Abstract**—Cadmium is a highly toxic heavy metal, and exposure to cadmium ions (Cd<sup>2+</sup>) can pose serious health risks to humans and the environment. Recent advancements in digital imaging have made high-resolution photo production from digital cameras more cost-effective, opening opportunities for rapid and affordable colorimetric methods in quantitative chemical analysis. The method employs the prime color space RGB (Red-Green-Blue) with individual values varying from 0 to 255. RGB data were extracted from square-homogenous cropped digital images using ImageJ software to construct a calibration curve in quantitative determination. TEM analysis confirmed the synthesis of mostly spherical AuNPs. FTIR data showed peaks at 3,442, 1,579, and 1,347 cm<sup>-1</sup> corresponding to the O-H, C=O, and C-O symmetric stretching vibrations of the -COOH groups on the surface of the synthesized AuNPs. XRD analysis revealed peaks at 38.3, 43.5, 64.6, 77.7, and 81.7°, confirming the crystalline nature of the AuNPs. The presence of cadmium causes the nanoparticles to aggregate, resulting in a color change from red (520 nm) to blue (650 nm), which can be analyzed using digital image methods. The method has good selectivity and sensitivity, with a detection limit of 0.050 ppm and a linear range from 0 to 10 ppm (R<sup>2</sup> = 0.9952). Therefore, this method can be successfully employed for detecting and quantifying unknown concentrations of cadmium.

**Keywords**—colorimetry, digital image, gold nanoparticles, cadmium

## I. INTRODUCTION

Water pollution is one of the significant environmental issues, both regionally and globally [1]. Water, containing organic components, is essential for various uses. However, industrial waste, rich in polluting metals, poses severe and persistent environmental challenges. Heavy metals, which are toxic substances posing a danger upon exceeding certain thresholds when entering the human body [2], tend to accumulate and resist natural decomposition within the body [3]. Chemical elements categorized as heavy metals exhibit a specific gravity greater than 5 gr/cm<sup>3</sup> and possess atomic numbers ranging from 22 to 92 [4]. Among the heavy metal ions frequently detected in water bodies are cadmium (Cd), lead (Pb), and mercury (Hg) [5].

Cadmium, an extraneous heavy metal characterized by elevated toxicity, exerts deleterious impacts on the physiological systems of the human body [4, 6]. The stipulated quality criterion according to South Sulawesi Government Regulation Number 82 of 2,001 for Cadmium (Cd) is 0.001 mg/L [1]. Cadmium possesses the capacity to induce impairment in diverse human physiological systems, augmenting susceptibility to breast cancer, cardiovascular diseases, respiratory disorders, and cardiac conditions. Moreover, cadmium toxicity has the potential to induce renal failure, gout, arthritis, and skeletal damage. Additionally,

exposure to Cadmium may detrimentally affect the reproductive glands and olfactory system, and even precipitate bone fragility [7–9]. Considering these ramifications, the identification of Cadmium (Cd) presence in water assumes paramount importance in averting the potentially fatal hazards it poses.

The analysis of cadmium can be accomplished through the utilization of specialized instrumentation, such as Atomic Absorption Spectrometry (AAS), Inductively Coupled Plasma-Atomic Emission Spectrometry (ICP-AES), Inductively Coupled Plasma-Mass Spectrometry (ICP-MS), Flame Atomic Absorption Spectrometry (FAAS), Graphite Furnace Atomic Absorption Spectroscopy (GFAS), and spectrophotometry [10–14]. These methodologies confer various advantages, encompassing sensitivity, selectivity, stability across diverse pH and thermal conditions, precision, and accuracy. However, the application of these methods is associated with elevated analysis costs and maintenance expenses that may be economically burdensome, necessitate specialized expertise for operation, and prove impractical for field analysis, thereby compromising the efficacy of detecting and monitoring cadmium exposure. Consequently, an alternative methodology is imperative; one that exhibits commendable sensitivity and selectivity, is cost-effective, and facilitates portability.

In recent times, there has been a heightened focus on developing colorimetric methods based on gold nanoparticles due to their simplicity, cost-effectiveness, portability, and practicality. Gold nanoparticles possess unique optical properties, which contribute to a more sensitive and selective detection system. These nanoparticles optical characteristics facilitate the creation of distinct colors for colorimetric detection applications, allowing visual observation by the naked eye [15]. This aspect is associated with their distinctive feature known as Localized Surface Plasmon Resonance (LSPR), a trait that emerges due to the collective oscillation of electrons in the conduction band following the interaction between AuNPs and electromagnetic radiation [16]. The fundamental principle behind the AuNPs-based colorimetric method lies in the aggregation capability of AuNPs. During aggregation, interactions among nanoparticle surfaces induce interparticle plasmon coupling, causing a shift in the LSPR towards longer wavelengths and broadening of the peak [17]. To enhance the selectivity of the colorimetric sensor, modifications were made to the gold nanoparticles using glutathione.

The quantitative analysis of cadmium metal utilizing gold nanoparticles as a colorimetric indicator can be conducted through digital image methods [18]. RGB data were extracted

from digital images, which were segmented into uniform square sections using ImageJ software, serving as the foundation for constructing calibration curves in quantitative determinations. The process of digital image analysis involved assessing the intensity of the R, G, and B color components of AuNPs after the addition of cadmium. The determination of cadmium concentration using digital images was accomplished using the Simple Linear Regression (SLR) calculation technique [19]. Based on these procedures, researchers developed a digital image-based colorimetric method for detecting cadmium metal.

## II. LITERATURE REVIEW

### A. Synthesis of Gold Nanoparticles (AuNPs)

The synthesis of AuNPs was first conducted by Turkevich in 1951, which remains the most used method. In this approach, the general approach in creating gold nanoparticle colloids involves synthesizing particles from HAuCl<sub>4</sub> using a reducing agent. AuNPs are synthesized with the Turkevich method using the reducing agent sodium citrate. The developed method involves adding sodium citrate to boiling gold ions, where sodium citrate acts as a reducing agent and a capping agent. This method produces spherical gold nanoparticles with a size of 20 nm. The chemical coordination occurring in AuNPs synthesized using the Turkevich method. Au<sup>3+</sup> aggregates to form AuNP, sodium citrate reduces Au<sup>3+</sup>, and then citrate is oxidized to form dicarboxyacetone. Dicarboxyacetone can stabilize the formed AuNPs.

### B. AuNPs based Colorimetric Sensor

Nanomaterials have gained widespread use in biosensing due to their advantageous characteristics, offering low detection limits and high sensitivity [20]. Among these, gold nanoparticles (AuNPs) serve as prominent colorimetric reporters owing to their substantial extinction coefficients and size-dependent optical properties, attracting attention for their robust light absorption in the visible spectrum, primarily driven by the Local Surface Plasmon Resonance (LSPR) [21]. LSPR, an optical phenomenon arising from the interaction between electromagnetic waves and a metal's conduction electrons, leads to the resonant oscillation of these electrons in gold nanostructures when exposed to light irradiation. The resonance frequency of this LSPR is highly influenced by various factors such as size, shape, interparticle interactions, dielectric properties, and the local environment (refractive index) of the nanoparticles. The detection mechanism relies on the presence of target analytes that induce either aggregation or redispersion of the gold nanoparticles, resulting in a discernible color change from red to blue or vice versa [22].

### C. Colorimetric based on SPR Change for Detection of Cadmium (II) ions

Many studies have reported the detection of heavy metal ions such as cadmium (II) ions based on their specific aptamers. For instance, a smartphone-linked colorimetric setup employing aptamer-functionalized AuNPs to identify cadmium (II) ions even in the presence of sodium chloride. The addition of an aptamer to the AuNPs solution notably bolstered their stability, averting aggregation. Upon

introducing cadmium (II) ions, the specific interaction between aptamers and these ions diminished the unbound aptamers, weakened the stability of AuNPs, and induced a visible change in the solution's color. This color variation could be rapidly recorded and analyzed within a brief span of 10 minutes using a newly developed Self-engineered Colorimetric Sensor (SBCS) designed explicitly for the quantitative detection of cadmium (II) ions.

Additionally, apart from the NaCl solution, the presence of PDDA (polydiene dimethyl ammonium chloride) also results in the aggregation of AuNPs, inducing a noticeable alteration in the solution's color. The electrostatic interaction between PDDA and aptamers in the solution initiates the formation of AuNPs-free particles, maintaining the solution's wine-red color. Nevertheless, when the aptamer binds to Cd (II) ions and unbound PDDA aggregates AuNPs, this interaction causes the solution to transition to a blue hue in the presence of Cd (II) ions. This color change can be effectively detected using a smartphone.

## III. MATERIALS AND METHODS

### A. Materials

Chloroauric acid (HAuCl<sub>4</sub>·3H<sub>2</sub>O), trisodium citrate dihydrate, (Na<sub>3</sub>C<sub>6</sub>H<sub>5</sub>O<sub>7</sub>·2H<sub>2</sub>O) glutathione reduced (C<sub>10</sub>H<sub>17</sub>N<sub>3</sub>O<sub>6</sub>S). The metal salts cadmium chloride (CdCl<sub>2</sub>), calcium chloride (CaCl<sub>2</sub>), manganese chloride (MnCl<sub>2</sub>), magnesium chloride (MgCl<sub>2</sub>), barium chloride (BaCl<sub>2</sub>), mercuric chloride (HgCl<sub>2</sub>), chromium trichloride (CrCl<sub>3</sub>), ferrous chloride (FeCl<sub>2</sub>), copper sulphate pentahydrate (CuSO<sub>4</sub>·5H<sub>2</sub>O), nickel chloride (NiCl<sub>2</sub>), cobalt chloride (CoCl<sub>2</sub>) procured from Sigma Aldrich.

### B. Synthesis of Gold Nanoparticles capped Glutathione

The AuNPs were synthesized using Turkevich method [23]. Trisodium citrate was used for the reduction of gold chloride trihydrate solution (HAuCl<sub>4</sub>). It also acted as the stabilizing agent for the synthesized AuNPs. The brief methodology includes heating of 35 mL of 100 ppm HAuCl<sub>4</sub> was mixed with 2 mL of 100 μM glutathione and stirred for 5 minutes. Subsequently, 5 mL of 0.25% sodium citrate was added, and the mixture was stirred for 60 minutes. The faint yellow colored solution turned to a bright ruby-red color indicating the reduction of gold ions to AuNPs. The SPR spectrum of the solution was measured using a spectrophotometer UV-Vis at wavelengths ranging from 350 to 850 nm.

### C. Characterization

The synthesized AuNPs were characterized by X-Ray Diffraction, Fourier Transform Infrared (FTIR), and Transmission Electron Microscope (TEM). Determination of the maximum absorbance value was measured using UV-Vis spectrophotometry.

### D. Colorimetric Assays Using AuNPs

For the colorimetric sensing of cadmium, 0.2 mL of different concentrations of cadmium ranging from 0 to 10 ppm was added to 0.6 ml of GSH-AuNPs solution and gently mixed. The mixture was allowed to react and observe any visible change in color. The UV—Visible absorbance of the solution was measured between 350 and 800 nm. The color

intensity was determined with ImageJ application.

#### E. Selectivity Assay for the Detection of Cadmium

To investigate the selectivity of the GSH-AuNPs reaction with cadmium, the metal ions  $\text{Cd}^{2+}$ ,  $\text{Ca}^{2+}$ ,  $\text{Mn}^{2+}$ ,  $\text{Mg}^{2+}$ ,  $\text{Ba}^{2+}$ ,  $\text{Hg}^{2+}$ ,  $\text{Cr}^{3+}$ ,  $\text{Fe}^{2+}$ ,  $\text{Fe}^{3+}$ ,  $\text{Na}^{2+}$ ,  $\text{Pb}^{2+}$ ,  $\text{Zn}^{2+}$ ,  $\text{Cu}^{2+}$ ,  $\text{Ni}^{2+}$ ,  $\text{Co}^{2+}$  were tested with the AuNPs under the same conditions at a concentration of 10 ppm. The solutions were monitored for any visual color change and the color intensity was determined with ImageJ application.

#### F. Quantification of the Digital Image

A digital image from the smartphone camera serves as a spectrophotometer analyzing the light passing through the colloid of the AuNPs. The average RGB color values were extracted from the image using ImageJ software. The raw plot of the RGB color values against the concentration of the standards, produces a hyperbolic trend. To obtain a linear plot for further usage, the initial RGB color values were converted to logarithmic scale following the Lambert–Beer law derivation formula as follows [23]:

$$I_R = \log \frac{R_0}{R_s}; I_G = \log \frac{G_0}{G_s}; I_B = \frac{B_0}{B_s} \quad (1)$$

$I_R$ ,  $I_G$  and  $I_B$  are the (color) intensity or absorbance for red, green, and blue, respectively. The terms  $(\text{RGB})_0$  and  $(\text{RGB})_s$  are the RGB color values of the blank and the sample, respectively. Here, the term ‘intensity’ refers to the number of R, G and B color values of the digital image, and thus is different from that used in UV-visible spectrophotometry. The logarithmic conversion of RGB color values is directly proportional to the cadmium ion concentration, so it can be used for the quantification of cadmium ions in the samples.

## IV. RESULT AND DISCUSSION

### A. Synthesis and Characterization of AuNPs

#### 1) UV-Visible spectroscopy and TEM analysis

Characterization was performed to assess the properties of the synthesized AuNPs. Typically, AuNPs manifest a distinctive absorbance spectrum within the 500–550 nm range, detectable through UV-Vis spectrophotometry. The verification of AuNPs formation involved visual observation and assessment based on UV-Vis absorption spectra synthesized under optimal conditions. The resultant high-quality AuNPs colloid exhibited a red hue, featuring a singular SPR absorption peak at a wavelength of 522 nm (Fig. 2(a)). The shift in the colloid’s color, transitioning from yellow to red, indicates the successful formation of AuNPs. This color change is ascribed to the excitation of surface plasmon vibrations on the metal nanoparticles, signifying both the reduction reaction from  $\text{Au}^{3+}$  to  $\text{Au}^0$  and the formation of AuNPs.

The gold nanoparticles, synthesized under optimal conditions, were subsequently modified with glutathione (GSH). This modification involved the addition of 2 mL of glutathione during the synthesis process. Spectral analysis reveals that gold nanoparticles modified with glutathione exhibit UV-Vis absorption spectra with a wavelength peak at 522 nm, while those without glutathione display UV-Vis absorption spectra with a wavelength peak at 521 nm.

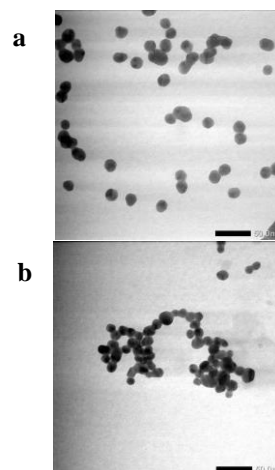
However, the spectral analysis indicates a slight decrease in the peaks but narrower spectra for the modified nanoparticles. This observation suggests that the modification with glutathione yields gold nanoparticles with a more uniform size distribution. In addition to the spectral changes, the modified gold nanoparticles appear to have a brighter color compared to those without modification.

The gold nanoparticles, synthesized under optimal conditions, were subsequently modified with glutathione (GSH). This modification entailed the addition of 2 mL of glutathione during the synthesis process. Spectral analysis reveals that gold nanoparticles modified with glutathione exhibit UV-Vis absorption spectra with a wavelength peak at 522 nm, while those without glutathione display UV-Vis absorption spectra with a wavelength peak at 521 nm. However, the spectral analysis indicates a slight decrease in the peaks but narrower spectra for the modified nanoparticles. This observation suggests that the modification with glutathione yields gold nanoparticles with a more uniform size distribution. In addition to the spectral changes, the modified gold nanoparticles appear to have a brighter color compared to those without modification.

The results of nanoparticle synthesis under optimal conditions were evaluated for their morphological characteristics and size distribution utilizing Transmission Electron Microscopy (TEM). As depicted in Fig. 1(a), it is apparent that the glutathione-modified AuNPs, successfully synthesized, demonstrate a consistent spherical shape, and are dispersed over a relatively wide spatial range. This dispersion is attributed to the absence of any aggregating substance among the AuNPs, facilitating the maintenance of particle dispersion.

#### 2) FTIR and XRD analysis

The broad absorption observed at approximately  $3,442 \text{ cm}^{-1}$  is attributed to the vibrational mode of hydroxyl groups present in water, citrate, and glutathione. Following the synthesis of AuNPs, the resulting colloids underwent a drying process in an oven at  $50^\circ\text{C}$  to remove water molecules. However, the solid AuNPs (powder) obtained post-drying exhibited a notable tendency to absorb moisture from the surroundings, known as high hygroscopicity. ATR-FTIR testing was conducted without vacuum conditions, leading to the retention of moisture in the solid AuNPs samples under analysis. Consequently, the -OH absorption peak appears around  $3,442 \text{ cm}^{-1}$ , indicating the continued presence of water molecules.



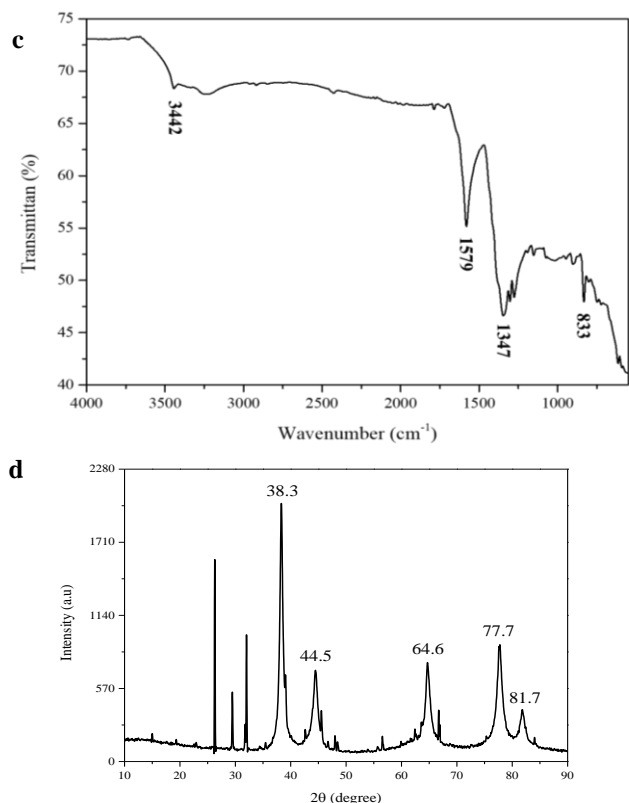


Fig. 1. (a) TEM image of GSH-AuNPs and (b) GSH-AuNPs-cadmium; (c) FTIR spectrum of the GSH-AuNPs; (d) The XRD patterns of GSH-AuNPs.

The absorptions observed at 1,579 and 1,347  $\text{cm}^{-1}$  correspond to the C=O and C-O symmetric stretching vibrations of the -COOH groups present in citrate and glutathione, respectively, while the absorption at 833  $\text{cm}^{-1}$  represents the C-C vibration (Fig. 1(c)). The presence of citrate and glutathione molecules on the surface of AuNPs serves two significant functions. Firstly, it aids in achieving chemical stability by reducing the surface energy of highly reactive AuNPs. Secondly, it functions to stabilize the AuNPs, thus preventing agglomeration and maintaining their well-distributed state, crucial for interactions with other molecules.

The GSH-modified AuNPs exhibit five characteristic peak types at  $2\theta$ , specifically confirmed at 38.3, 43.5, 64.6, 77.7, and 81.7° (Fig. 1(d)), corresponding to the standard Bragg reflections of 111, 200, 220, 311, and 222, suggesting the face-centered cubic lattice structure of the synthesized AuNPs and confirming their crystalline nature, respectively (JCPDS file No. 00-004-0784). Notably, the XRD peak in the (111) plane is more predominant compared to the peaks in the 200, 220, 311, and 222 planes. This prevalence can be attributed to the preference of AuNPs crystals to occupy the (111) plane.

### B. Reaction between GSH-AuNPs and Cadmium

As the concentration of  $\text{Cd}^{2+}$  increases, there is an augmentation in the coordination between  $\text{Cd}^{2+}$  and the carboxylate groups of citrates and GSH. This escalation results in the formation of complexes involving  $\text{Cd}^{2+}$ , GSH via the free sulfhydryl group, and carboxyl groups. This molecular interaction brings AuNPs into proximity, leading to a state of weak electrostatic repulsion and robust electrostatic interparticle interactions among the AuNPs.

Theoretical propositions and experimental validations support the concept that the plasmon oscillation of metal nanoparticles couples when they are in proximity. The nearness of AuNPs induces the coupling of their plasmon oscillation, inducing a bathochromic shift in the absorption band, a reduction in zeta potential, and consequently, aggregation. Due to the substantial size increase during aggregation, the LSPR wavelength experiences an increment with the rise in particle size, a consequence of near-field coupling in the resonant wavelength peak of the interacting particles.

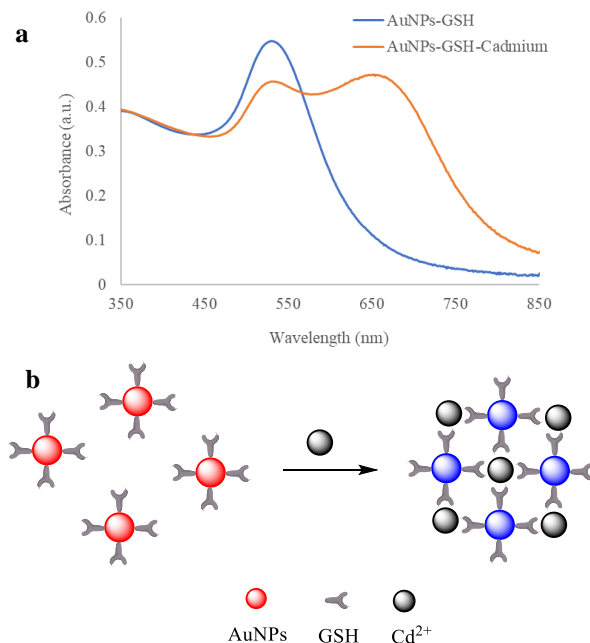


Fig. 2. (a) UV-visible absorption spectra of AuNPs before and after added cadmium; (b) Schematic diagram of reaction between AuNPs and cadmium ion.

The mechanism of GSH-AuNPs aggregation after the addition of  $\text{Cd}^{2+}$  is illustrated graphically in (Fig. 2(b)), which displays the absorption spectra of GSH-AuNPs. This analysis was conducted to assess the practical feasibility of employing them in the environment for detecting  $\text{Cd}^{2+}$ . The absorbance at 520 nm increased, and a new absorption band around 650 nm emerged (Fig. 2(a)). This observation is supported by the TEM data shown in Fig. 1(c). The aggregation of GSH-AuNPs resulted in a change in the Localized Surface Plasmon Resonance (LSPR) of the AuNPs, leading to the development of a blue color due to interparticle plasmon coupling. The change in LSPR is influenced by the size, morphology, interparticle distance, and extent of aggregation of the AuNPs.

### C. Digital Image-based Colorimetric Detection of Cadmium

In the presence of varying concentrations of cadmium ranging from 0 to 10 ppm in the AuNP solution, a gradient of different color changes was observed (Fig. 3(a)). The color of the AuNP solution shifted to blue as the concentration of cadmium increased, ultimately yielding a blue color at 10 ppm. For the quantitative measurement of cadmium in the AuNPs solution, a standard calibration curve was plotted using standard cadmium concentrations against the color intensity of the solution, ranging from 0 to 10 ppm in AuNPs solution. The standard calibration curve exhibited a linear

relationship between the cadmium concentration and the absorbance, with a reliable  $R^2$  value of 0.9952 in the selected range (Fig. 3(b)). The detection limit was calculated to be 0.050 ppm based on the signal-to-noise ratio (S/N) of 3. Therefore, this method can be successfully employed for the detection and quantification of unknown concentrations of cadmium.

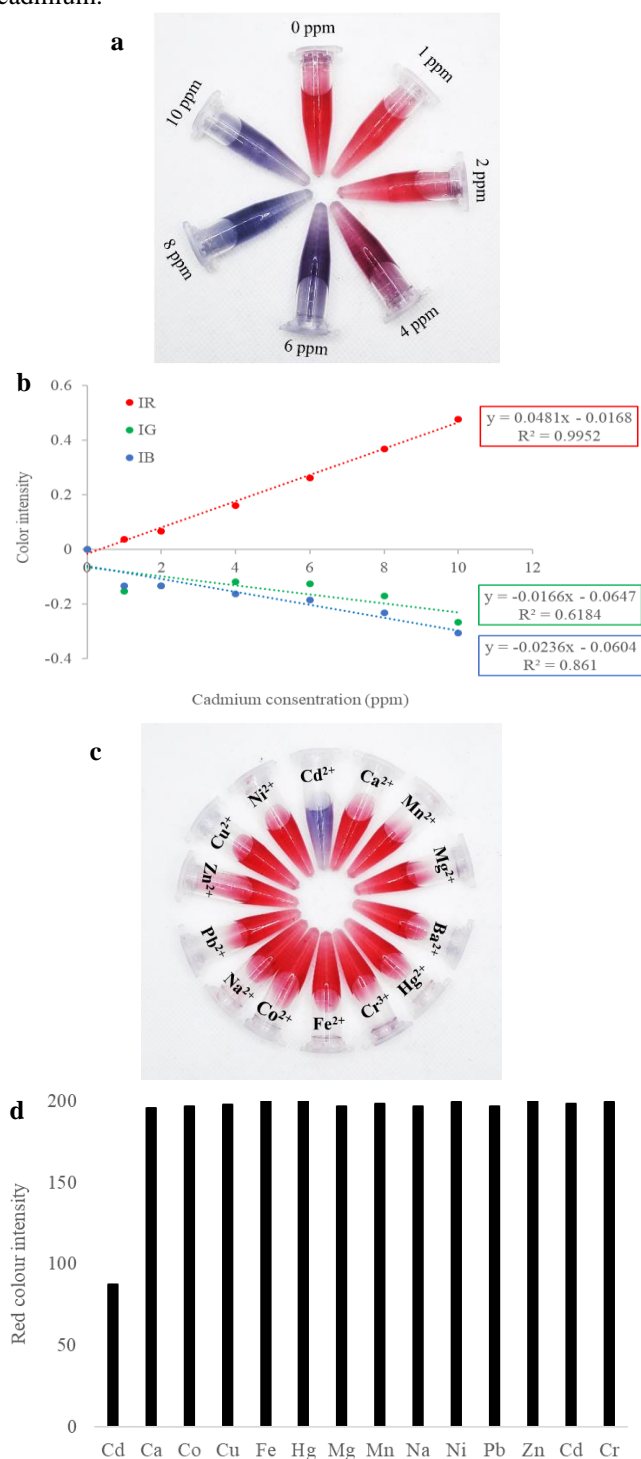


Fig. 3. (a) Photograph of the GSH-AuNPs with different concentrations of cadmium; (b) Calibration curve of cadmium detection from 0 to 10 ppm; (c) The corresponding color change photo image of GSH-AuNPs added with different metal ion showing selectivity; (d) Red color intensity of AuNPs in the presence of cadmium or other interferences.

#### D. Selectivity Assay for the Detection of Cadmium

The colorimetric selectivity test of the GSH-AuNPs probe, supported by the color of the AuNP solution, remained unchanged and stable even after 24 hours, indicating the high

selectivity and specificity of the AuNPs towards cadmium (Fig. 3(c)). To further confirm the selectivity of the assay, the color intensity of the AuNPs solution in the presence of cadmium (10 ppm) was investigated. The color intensity in Fig. 3(d) of GSH-AuNPs containing  $\text{Cd}^{2+}$ ,  $\text{Ca}^{2+}$ ,  $\text{Mn}^{2+}$ ,  $\text{Mg}^{2+}$ ,  $\text{Ba}^{2+}$ ,  $\text{Hg}^{2+}$ ,  $\text{Cr}^{3+}$ ,  $\text{Fe}^{2+}$ ,  $\text{Fe}^{3+}$ ,  $\text{Na}^{2+}$ ,  $\text{Pb}^{2+}$ ,  $\text{Zn}^{2+}$ ,  $\text{Cu}^{2+}$ ,  $\text{Ni}^{2+}$ ,  $\text{Co}^{2+}$  ions (0.5 mL, 10 ppm) demonstrates that cadmium exhibited significantly lower red intensity color values compared to the other tested analytes, indicating that these substances do not interfere with this assay. Thus, the GSH-AuNPs-based colorimetric assay was expected to be employed as a selective colorimetric visual probe for cadmium.

## V. CONCLUSION

We have reported the developed method allows a colorimetric detection of cadmium ranging from 0–10 ppm yielding different colors based on the concentration of cadmium where the degree of aggregation of GSH-AuNPs is linearly proportional to the concentration of cadmium. The GSH-AuNPs sensor exhibited a linear correlation between the red color intensity and cadmium concentration ( $R^2 = 0.9952$ ), and a low detection limit of 0.050 ppm. The advantages of a very simple, sensitive, and highly selective approach utilizing GSH-AuNPs for the qualitative and quantitative detection of cadmium. Future research would be enhanced by integrating the colorimetric sensor into paper, enabling its use anytime and anywhere.

## AUTHOR CONTRIBUTIONS

Eduwin Saputra: Conducted the research, validation, formal analysis, investigation, and writing the original draft.

Sri Juari Santosa: Validation, formal analysis, writing-review, and editing.

## FUNDING

This research was funded by the Indonesia Endowment Fund for Education (LPDP) under the Ministry of Finance, Indonesia.

## ACKNOWLEDGMENT

This research was funded by the Indonesia Endowment Fund for Education (LPDP) under the Ministry of Finance, Indonesia and Universitas Gadjah Mada for funding this conference.

## CONFLICT OF INTEREST

The authors declare no conflict of interest.

## REFERENCES

- [1] K. N. Jais, M. Ikhtiar, A. Gafur, H. H. Abbas, and Hidayat, "Bioaccumulation of Cadmium (Cd) and Chromium (Cr) heavy metals in water and Fish in Tallo Makassar River," *Window of Public Health Journal*, vol. 3, pp. 261–274, 2020. doi: 10.33096/woph.v1i13.65 (in Indonesian)
- [2] I. Hananingtyas, "Pollution study of heavy metals lead (Pb) and Cadmium (Cd) in Tuna fish (*Euthynnus* sp.) on the north coast of Java," *The Journal of Tropical Biology*, vol. 2, pp. 41–50, 2017. <https://jurnalsaintek.uinsa.ac.id/index.php/biotropic/article/view/132> (in Indonesian)
- [3] I. Yulianti, S. S. Edy, B. A. Saputra, M. P. Aji, Susanto, and Kurdi. "Detection of Cadmium ion by evanescent wave based Chitosan coated optical fiber sensor," *Journal of Physics*, pp. 1–6, 2017.

- [4] A. Sasongko, K. Yulianto, and Sarastri, "Verification of the method for determining Cadmium (Cd) metal in domestic wastewater using the atomic absorption spectrophotometry method," *Jurnal Sains dan Teknologi*, vol. 6, pp. 228–237, 2019. doi: 10.23887/jstundiksha.v6i2.10699 (in Indonesian)
- [5] I. Vaezuza, K. E. Kurniansyah, F. Darma, and I. Yulianti, "Plastic fiber optic sensor fabrication for detection of mercury metal ions in water," *Komunikasi Fisika Indonesia*, vol. 16, pp. 123–129, 2019. doi: 10.31258/jkfi.16.2.123-129 (in Indonesian)
- [6] L. Firdaus and Anurohim, "The effect of giving Carboxymethyl Chitosan (KMK) in efforts to reduce levels of the heavy metal Cadmium (Cd) in green mussels (*Perna viridis* Linn.) from the waters of Lamong Bay, Surabaya," *Jurnal Sains dan Seni ITS*, vol. 8, pp. 23–30, 2019. doi: 10.12962/j23373520.v8i2.48606 (in Indonesian)
- [7] F. Istarani and E. Pandebesie, "Study of the impact of arsenic (As) and cadmium (Cd) on environmental quality degradation," *Jurnal Teknik Pomits*, vol. 3, pp. 2337–3539, 2014. doi: 10.12962/j23373539.v3i1.5684 (in Indonesian)
- [8] M. R. Ullah and M. E. Haque, "Spectrophotometric determination of toxic elements (cadmium) in aqueous media," *Journal of Chemical Engineering*, vol. 25, pp. 1–12, 2010.
- [9] A. M. L. Marzo, J. Pons, D.A. Blake, and A. Merkoçl, "All-integrated and highly sensitive paper-based device with sample treatment platform for Cd<sup>2+</sup> immunodetection in drinking/tap waters," *Analytical Chemistry*, vol. 85, pp. 3532–3538, 2013.
- [10] K. Ong. (2014). Determination of lead and Cadmium in foods by graphite Furnace atomic absorption spectroscopy. [Online]. Available: [www.perkinelmer.com](http://www.perkinelmer.com).
- [11] H. Cesur and B. Bati, "Determination of cadmium by FAAS after solid-phase extraction of its 1-benzylpiperazinedithiocarbamate complex on microcrystalline naphthalene," *Turkish Journal of Chemistry*, vol. 26, pp. 29–35, 2002.
- [12] J. P. Rawat, U. Nasaer, and S. M. A. Andrabi, "Chelation ion chromatography on alizarin red S loaded rannic silicate-selective separation of Cd<sup>2+</sup> and Pb<sup>2+</sup> from some transition metal ions," *Indian Journal of Chemical Technology*, vol. 19, pp. 71–74, 2012.
- [13] S. Kulkarni, S. Dhokpande, and J. Kavar, "A Review on spectrophotometric determination of heavy metals with emphasis on cadmium and nickel determination by UV spectrophotometry," *International Journal of Advanced Engineering Research and Science*, vol. 2, pp. 2349–6495, 2015.
- [14] G. Jin, J. Kan, Y. Zhu, and N. Lei, "Spectrophotometric determination of cadmium (II) using the chromogenic reagent (4-O-diazoaminophenylarsonic acid) azobenzene," *Indian Journal of Chemistry*, vol. 39, pp. 1227–1230, 2000.
- [15] A. K. Parmar, N. N. Valand, K. B. Solanki, and S. K. Menon, "Picric acid capped silver nanoparticles as a probe for colorimetric sensing of creatinine in human blood and cerebrospinal fluid samples," *Analyst*, vol. 141, pp. 1488–1498, 2016.
- [16] L. A. Austin, M. A. MacKey, E. C. Dreaden, and El-Sayed, "The optical, photothermal, and facile surface chemical properties of gold and silver nanoparticles in biodiagnostics, therapy, and drug delivery," *Arch. Toxicol*, vol. 88, pp. 1391–1417, 2014.
- [17] M. T. Alula, L. Karamchand, N. R. Hendricks, and J. M. Blackburn, "Citrate-capped silver nanoparticles as a probe for sensitive and selective colorimetric and spectrophotometric sensing of creatinine in human urine," *Anal. Chim.*, vol. 1007, pp. 40–49, 2018.
- [18] M. L. Firdaus, W. Alwi, F. Trinoveldi, I. Rahayu, L. Rahmidar, and K. Warsito, "Determination of Chromium and iron using digital image-based colorimetry," *Procedia Environ*, vol. 20, pp. 298–304, 2014.
- [19] C. Purnomo, "Multiple Linear Regression and Simple Linear Regression Techniques for Heavy Metal Analysis in Digital Images Using Silver Nanoparticles as an Indicator," *S. Pd. Thesis, Dept. Edu., Universitas Bengkulu*, Bengkulu, Indonesia, 2016. (in Indonesian)
- [20] Q. U. A. Zahra, Z. Luo, R. Ali, M.I. Khan, F. Li, and B. Qi, "Advances in gold nanoparticles-based colorimetric for the detection of antibiotics," *An overview of the past decade Nanomaterials*, pp. 840, 2012.
- [21] W. Zhou, K. Hu, S. Kwee, L. Tang, Z. Wang, J. Xia, and X. J. Li, "Gold nanoparticle aggregation-induced quantitative photothermal biosensing using a thermometer: A simple and universal biosensing platform," *Anal. Chem*, vol. 92, pp. 2739–2747, 2020.
- [22] G. Liu, M. Lu, X. Huang, T. Li, and D. Xu, "Application of gold-nanoparticle colorimetric sensing to rapid food safety screening," *Sensors*, vol. 18, pp. 1–16, 2018.
- [23] J. Turkevich, P. C. Stevenson, J. Hillier, "A study of the nucleation and growth processes in the synthesis of colloidal gold," *Discuss. Faraday Soc.*, vol. 11, p. 55, 1951.

Copyright © 2024 by the authors. This is an open access article distributed under the Creative Commons Attribution License which permits unrestricted use, distribution, and reproduction in any medium, provided the original work is properly cited ([CC BY 4.0](https://creativecommons.org/licenses/by/4.0/)).